Research Square

Preprints are preliminary reports that have not undergone peer review.
They should not be considered conclusive, used to inform clinical practice,
or referenced by the media as validated information.

Controlling methanol feeding for recombinant protein production by *Pichia pastoris* under oxidation stress in fed-batch fermentation

Rongkang Hu
South China University of Technology
Dongming Lan
South China University of Technology
Ruiguo Cui
South China University of Technology
Haomin Hong
South China University of Technology
Yachun Niu
South China University of Technology
Yonghua Wang (yonghw@scut.edu.cn)
South China University of Technology https://orcid.org/0000-0002-8790-4357

Research

Keywords: High cell density fermentation, Reactive oxygen species, Oxidative damage, Cell viability, Glutathione

Posted Date: October 7th, 2020

DOI: https://doi.org/10.21203/rs.3.rs-85999/v1

License: This work is licensed under a Creative Commons Attribution 4.0 International License.
Read Full License

Abstract

Background: Methanol can be used by *Pichia pastoris* as the sole carbon source and inducer to produce recombinant proteins in high-cell-density fermentations, but also damages cells due to reactive oxygen species (ROS) accumulation from methanol oxidation. Here, we study the relationship between methanol feeding and ROS accumulation by controlling constant methanol feeding rate during the induction phase.

Results: Higher methanol feeding rate increased the level of ROS accumulation caused by methanol oxidation. While the cell growth rate was proportional to the rate of methanol feeding rate, but maximum total protein production and highest enzyme activity were achieved at methanol feeding rate 4 mL/(L·h) as compared to that with 5 mL/(L·h). Moreover, oxidative demage induced by over accumulation of ROS in *P. pastoris* during the methanol induction phase caused cell death and reduced protein expression ability. ROS scavenging system analysis reveals that the higher methanol feeding rate, especially 5 mL/(L·h), resulted in increased intracellular catalase activity and decreased glutathione content significantly. Finally, Spearman's correlation analysis further reveals that the reduced glutathione might be beneficial for maintaining cell viability and increasing protein production under oxidative stress caused by toxic accumulation of ROS accumulation.

Conclusion: Our findings suggest an integrated strategy to control the feeding of the essential substrate based on analyzing its response to oxidative stress caused by toxic accumulation of ROS accumulation, as well as develop strategy to optimize fed-batch fermentation.

Introduction

Methylotrophic yeast *Pichia pastoris* is one of the most extensively used expression systems for heterologous protein production [1–3]. Methanol serves both as a carbon source for yeast growth in high-cell-density fermentations of *P. pastoris* and an inducer to produce heterologous proteins [4, 5]. However, the accumulation of intracellular toxic byproducts from methanol oxidation may cause oxidative damage to cells [6]. High methanol levels lead to accumulation of intracellular toxic oxidative by-products such as formaldehyde to cause cell death, whereas low methanol levels reduce protein productivity by triggering proteolytic degradation of the recombinant protein [7, 8].

The shift from growth solely on glycerol to growth and heterologous proteins production on methanol has a drastic impact on yeast. Methanol provides a carbon skeleton for cell growth and target protein synthesis. Methanol entering in *P. pastoris* cell will be oxidized to formaldehyde in the peroxisome molecule and produces H_2O_2. H_2O_2 is known as reactive oxygen species (ROS). During the fermentation of *P. pastoris*, the accumulation of metabolic by-product (H_2O_2), methanol oxidation may cause oxidative damage to cells and may cause degradation of heterologous proteins [9]. Therefore, methanol concentration must be carefully controlled at an adequate range to achieve the best synergy between methanol consumption and cell growth [10–12]. To control methanol within an adequate range in fed-batch fermentation, methanol feeding is the only parameter to optimize.

Increasing the methanol consumption blindly may cause the accumulation of ROS and reduce methanol utilization. The stress response of cells to environmental stress is a basic regulation mode of microbial life activities. Feeding strategies regulate the cell growth and the heterologous proteins by affecting cell metabolism. Methanol feeding rate is relatively high in the high-density fermentation of *P. pastoris*. Similar to all other organisms, yeast cells have limited tolerance against oxidation stress, for example by enzymatic and non-enzymatic systems to respond ROS [13]. Methanol fed-batch results in higher stress levels of organelles for protein processing [14]. The unfolded protein response-regulated oxidative folding mechanism in the endoplasmic reticulum further leads to the accumulation of intracellular ROS [15]. Therefore, the methanol feeding strategy optimized by the parameters will be limited by the methanol-induced intracellular biological response network [16]. Exploration of future optimal induction modes from cell physiological and metabolic functions is the guarantee for large-scale production of heterologous proteins.

We applied constant methanol feeding strategies during the induction phase, and examined the effects of different constant methanol feeding rates on post-induction cell growth and ROS scavenging systems. We identified the correlation of fermentation conditions with ROS-associated parameters. Then we investigated the expressions profile of genes involved in ROS scavenging system at mRNA level. Our findings suggest an integrated strategy to control the feeding of the essential substrate based on analyzing its response to oxidative stress caused by toxic accumulation of ROS accumulation.

Results

Biomass, total protein concentration, lipase activity, alcohol oxidase activity

To examine the effects of different constant-rate methanol feeding rates on fermentation conditions, we kept the operating conditions of glycerol batch phase and glycerol fed-batch phase identical for all fermentations and only used different constant methanol feeding rates during the induction phase. For all fermentations, the residual methanol concentration was approximately zero throughout the induction phases.

As shown in Fig. 1A, the methanol feeding rate had direct impact on the cell growth rate and biomass. Higher methanol feeding rates led to greater cell growth. At postinduction times of 150, 126, 126 and 102 h, the attainable cell densities for the four rates were 392, 436 and 448 and 479 g/L wet cell density (WCD), respectively. Figure 1B and Fig. 1C shows the time courses of total protein concentration and lipase activity throughout the induction phase with different feeding rates. During the first 24 h after induction, protein production and lipase activity was similar for the four rates. However, maximum total protein concentration value and lipase activity reached were 2.78 g/L and 1166.5 U/mL for feeding rate of 4 mL/(L·h). Figure 1D illustrates time profiles of specific alcohol oxidase (AOX) activity based on WCD during methanol induction phase. The time required to reach the maximum specific AOX activity also varied with methanol feeding rate, and higher methanol feeding rates resulted in maximum specific AOX activity being achieved earlier.

Effects of methanol feeding rate on cell viability and cell death

Figure 2A shows the effect of methanol feeding rate on cell viability within the range of constant-rate methanol feeding rates 2–5 mL/(L·h) in a 5-L bioreactor. At all four rates, the cell activity decreased with the extension of induction time. Among the 2, 3 and 4 mL/(L·h), the flow rate showed an apparent flow rate-dependent positive effect on *P. pastoris* cell viability. The cell viability decreased significantly after 72 hours of induction for feeding rates of 2, 3 and 4 mL/(L·h). From the process point of 5 mL/(L·h), the transition of rapid decline in cell viability was advanced to 48 h after induction. Figure 2B shows that each group of cells had different amounts of red fluorescence after staining with propidium iodide. Normal cells could not be stained, the early apoptotic cells showed weak red fluorescence, the late apoptotic cells showed enhanced red fluorescence, and the dead cells showed strong red fluorescence. The number of cells showing propidium iodide-positive (red fluorescence) was higher at 5 mL/(L·h), and the cells mainly showed weak fluorescence intensity. Moreover, the percentage of propidium iodide-positive cells in other feeding rates showed lower red fluorescence, and most cells exhibited enhanced red fluorescence. From the above results, the 4 mL/(L·h) constant methanol feeding rate appears to be most preferable because it maintained the highest cell viability and the lowest level of cell death.

Effects Of Methanol Feeding Rate On ROS Accumulation

As shown in Fig. 3, the accumulation levels of $O_2^{\bullet-}$ and H_2O_2 in *P. pastoris* cultured with four constant methanol feeding rates were different. Four methanol feeding rates did not cause a significant increase in $O_2^{\bullet-}$ content in *P. pastoris*. However, *P. pastoris* had higher cellular $O_2^{\bullet-}$ levels with 5 mL/(L·h) in the induction phase compared with that in other methanol feeding rate induction conditions. Moreover, higher methanol feeding rates resulted in increased cellular H_2O_2 levels. Notably, for 5 mL/(L·h) constant methanol feeding rate, the cellular H_2O_2 and ROS accumulation levels were significantly higher than other induction groups. For example, the cellular H_2O_2 and ROS accumulation levels reached were 2.4 nmol/min/mg-WCD, and 1041 FLU/10^6 cells for feeding rates of 5 mL/(L·h), respectively. However, the cellular H_2O_2 and ROS accumulation levels being 1.0 nmol/min/mg-WCD and 563 FLU/10^6 cells at methanol feeding rates of 4 mL/(L·h), respectively. We ran the fermentation with the 3 and 4 mL/(L·h) methanol feeding rates. Compared to 3 mL/(L·h), the feeding rate of 4 mL/(L·h) yielded a slight increase in cellular H_2O_2 and ROS accumulation levels.

Effects of methanol feeding rate on cellular ROS scavenging system

We assayed activities of superoxide dismutase (SOD) and catalase (CAT), and the content of reduced glutathione (GSH). Unexpectedly, except the increase of CAT activity, the results showed that higher methanol feeding rates caused nearly no change of SOD activity, and an obvious decrease in concentration of GSH with 5 mL/(L·h) (Table 1). Moreover, the CAT activity with a methanol feeding rate of 4 mL/(L·h) showed no comparable difference with that 3 mL/(L·h), whereas the CAT activity in with methanol feeding rate of 5 mL/(L·h) increased obviously.

Table 1
Cellular ROS scavenging system in fed-batch fermentation by *Pichia pastoris* under different methanol feeding rates

Methanol feeding rate (mL/(L·h))	SOD (U/mg-protein)	CAT (U/mg-protein)	GSH (mg/g-WCD)
2	1.8 ± 0.2	1.1 ± 0.1	3.5 ± 0.2
3	1.7 ± 0.1	1.6 ± 0.2	3.2 ± 0.3
4	1.9 ± 0.2	1.8 ± 0.1	3.0 ± 0.3
5	2.0 ± 0.1	2.7 ± 0.3	0.8 ± 0.2

Effects Of Methanol Feeding Rate On Lipid Peroxidation

The malondialdehyde (MDA) levels were determined in order to evaluate oxidative damage in the cell of recombinant *P. pastoris* exposed to four methanol feeding rates (Fig. 4). All the cultures analyzed showed difference after induction with four methanol feeding rates comparison to the 0 h, indicating that there was a change in the production of lipid peroxidation of recombinant *P. pastoris*. The MDA levels were similar for the methanol feeding rates of 2, 3 and 4 mL/(L·h) at the end of fermentation. By contrast, 5 mL/(L·h) at 96 h showed a significant higher MDA level with respect to the other induction groups.

Correlation Of Fermentation Performance With Ros-associated Parameters

Figure 5 gives the heatmap constructed by Spearman's correlation analysis, to explore the correlations of fermentation performance and with ROS-associated parameters. The relevant parameters causing the accumulation of ROS in *P. pastoris* cells were related to the methanol feeding rate. Generally, high cell biomass and higher cell viability were beneficial for increasing total protein content and lipase activity. However, cell viability was negatively correlated with the cell biomass. Therefore, methanol feeding rate must be carefully controlled at an adequate range to achieve the best synergy between cell viability and cell growth. Once the balance between cell viability and cell growth was disturbed, it led to a decrease in GSH level. In addition, the ROS accumulation level that affects total protein concentration and enzyme activity was closely related to cell viability. Those interventions were further regulated by GSH levels. For this purpose, the prerequisite is to understand how methanol feeding affects the changes in GSH levels in high cell density fermentation.

RT-qPCR analysis of intracellular gene expression

Figure 6 shows that the ROS scavenging system related gene was amplified from the cDNA, and all samples were compared with methanol feeding rate 3 mL/(L·h). Figure 6 shows that higher methanol feeding rates caused a down-regulation of cytosolic superoxide dismutase (cSOD), glutathione peroxidise (GPX1) and glutathione reductase (GLR1) at the mRNA levels. CAT expression at the mRNA level was higher for feeding rates of 4 and 5 mL/(L·h) compared with that 3 mL/(L·h). Especially, 5 mL/(L·h) methanol feeding rate had a significantly higher expression of CAT at the mRNA level compared with that

3 mL/(L·h) ($p < 0.05$). Moreover, cSOD, GPX1 and GLR1 mRNA level was higher for feeding rates of 4 mL/(L·h) in the methanol inducted phase than that 5 mL/(L·h).

Discussion

P. pastoris is extensively used to produce various heterologous proteins. Amounts of biopharmaceutical drugs and industrial enzymes have been successfully produced by fed-batch high-cell-density fermentation of this cell factory. Although high-density fermentation of *P. pastoris* is considered as a promising development, it also has its limitations. It is not reliable to judge methanol concentration by dissolved O_2 alone in the fermenter, because the accumulation of intracellular toxic byproducts from methanol oxidation may cause cytotoxic to cells. Similar phenomenon happens for the production of growth hormone by *Lateolabrax japonicas* [17]. Therefore, it is necessary to seek more perfect methods to promote protein production based on reducing the accumulation of toxic by-products of methanol oxidation.

The rate of constant-rate methanol feeding had direct impact on the cell growth rate and cell biomass. The rate of 2 mL/(L·h) gave the lowest cell biomass. Compared to 3 and 4 mL/(L·h), the feeding rate of 2 mL/(L·h) yielded a lower total protein concentration and enzyme activity. These results indicate that lack of carbon/energy sources could not meet the sufficient requirements for the cell metabolism, and could also cause declines in cellular metabolic activity. For this reason, while cell viability at the methanol feeding rate of 2 mL/(L·h) was still similar after 72 h of induction, but the final value after 144 h induction was lower than that of 3 and 4 mL/(L·h) methanol feeding rate. By contrast, although the rate of 5 mL/(L·h) caused rapid accumulation of total protein concentration and enzyme activity during the first 96 h after induction. However, from the process of induction phase, the 3 and 4 mL/(L·h), especially 4 mL/(L·h) methanol feeding rate appears to be most preferable because it produces the highest total protein concentration and highest enzyme activity. Current research recognized that excessive methanol would damage the AOX1 transcriptional efficiency and cellular metabolic activity, particularly when cells are exposed to high methanol concentration for long time, as excessive methanol and dissolved oxygen may lead to accumulation of formaldehyde, the first intermediate of methanol metabolism, to certain toxic levels [9, 18, 19]. Our study showed that higher flow rate (5 mL/(L·h)) resulted in rapid decrease in cell activity. One reason might be that higher methanol toxicity maintained low cell viability. These conclusion and results could be found in related report [20]. However, we further investigated that the accumulation of ROS from methanol oxidation may cause oxidative damage to cells. Difference from the accumulation of formaldehyde to certain toxic levels, in this study, the decline in cell activity caused by oxidative damage was also considered as one of the crucial factors for the metabolic toxicity of methanol.

Accumulation of ROS in cells caused by higher methanol feeding rates can form oxidative damage. MDA is by-product of lipid peroxidation and reflect the degree of oxidative damage caused by ROS [13]. For 5 mL/(L·h) constant methanol feeding rate, the cellular ROS accumulation and MDA levels were significantly higher than other induction conditions, indicating that the higher methanol feeding rates led

to a significant increase in lipid peroxidation in *P. pastoris*. Generally, the cellular ROS scavenging system attenuate the oxidative damage by scavenging ROS, but excessive H_2O_2, which is not scavenging in time, can damage the lipids on the cell membrane [21]. Since membrane phospholipids are rich in unsaturated fatty acids and the hydrophobic membrane has high solubility for oxygen atoms, so it is most vulnerable to free radical [22]. So here we indeed found that the oxidative damage induced by accumulation of ROS at the methanol feeding rate of 5 mL/(L·h) can cause cell apoptosis at early stage and reduced protein expression ability.

Therefore, controlling intracellular ROS accumulation is benefic for improving protein production in *P. pastoris* during the methanol induction phase. Evidence from our study demonstrated that the methanol feeding rate of 4 mL/(L·h) can stabilize the ROS scavenging system. Notably, the ROS accumulation level that affects total protein concentration and enzyme activity was closely related to cell viability. Those interventions were further regulated by GSH levels. Other protein factors are also effective defense strategies to ameliorate the toxic effects of ROS, such as GPX1 and CAT. While GPX and CAT utilize H_2O_2 as substrate, GSH protects cells from oxidative stress and endogenous toxic metabolites through HCHO metabolism and detoxification of ROS [23]. Actually, GPX1 also acts as a prophylactic antioxidant enzyme, with GSH to attenuate ROS accumulation, and is converted from the oxidized (GSSG) to reduced form (GSH) by GLR1 [24]. In this study, instead of increase, the concentration of GSH decreased along with ROS accumulation, suggesting higher methanol feeding rates induced damage to cellar ROS scavenging system. Since GLR1 and GPX1 control the cycle of transition between GSH and GSSG, the significant high expression levels of their encoding gene expressions indicate smoothness of the transformation, thus explaining the reason for the high GSH content at methanol feeding rates of 2 mL/(L·h), 3 mL/(L·h) and 4 mL/(L·h). It was reported that p53 reactivation and induction of massive apoptosis (PRIMA-1Met) inducing myeloma cell death by impairing GSH/ROS balance in human myeloma cell lines [25]. Similarly, titanium dioxide nanoparticles might cause a PRIMA-1Met-like effect in *P. pastoris*, independent of titanium dioxide nanoparticles [26]. However, in this study, methanol acts as a carbon source and inducer for *P. pastoris*. We supposed that metabolic by-product (H_2O_2), methanol oxidation may cause the accumulation of ROS, and induce oxidative damage to cells via impairing ROS scavenging system, especially GSH system, thereby reducing protein expression ability.

Conclusions

Methanol-feeding as a crucial operating parameter increases heterologous protein productivity by *P. pastoris*, but the accumulation of intracellular toxic byproducts from methanol oxidation may cause oxidative damage to cells. Our study demonstrates that controlling the constant methanol feeding rate of 4 mL/(L·h) promoted protein production by selectively balancing ROS scavenging system and reducing oxidative damage to cells. Importantly, methanol feeding rate within suitable range can maintained a high content of GSH. Our findings help understand methanol-induced intracellular bioreaction network in high-cell-density fermentation. This strategy may serve as reference for similar fermentation processes.

Materials And Methods

Strain and chemicals

P. pastoris X-33 strain (Invitrogen, Carlsbad, CA) was transformed with plasmid pPICZα A containing the lipase MAS1 gene. Lipase MAS1 gene expression was regulated by the AOX1 promoter [27, 28]. Yeast extract peptone dextrose (YPD) medium for seed culture contained (g/L) yeast extract 10.0, peptone 20.0 and glucose 20.0. The basal salt medium (BSM) for batch fermentation contained (g/L) glycerol 40, 85% H_3PO_4 26.7 mL, $CaSO_4$ 0.93, K_2SO_4 18.2, $MgSO_4{\cdot}7H_2O$ 14.9, KOH 4.13, PTM_1 salt solution 4.35 mL. PTM_1 salt solution contained (g/L) $CuSO_4{\cdot}5H_2O$ 6, NaI 0.08, $MnSO_4{\cdot}4H_2O$ 3, $ZnSO_4{\cdot}7H_2O$ 20, $FeSO_4{\cdot}7H_2O$ 65, $CoCl_2{\cdot}6H_2O$ 0.5, boric acid 0.02, H_2SO_4 5 mL. All other chemicals of analytical grade were supplied from Sinopharm Chemical Reagent Co., Ltd (Shanghai, China) unless otherwise indicated.

Seed Culture

The first inoculum culture was prepared from one colony of *P. pastoris* suspended in 50 mL sterilized YPD broth containing 100 μg/mL zeocin (Invitrogen, Carlsbad, CA). The culture was incubated at 30 °C in a 500-mL baffled shake-flask on rotary shaker at 250 rpm. After the OD_{600} reaches 2–6 in 18–24 h, a second inoculum culture was prepared by transferring the first inoculum 10 (v/v) into a 2-L baffled shake-flask containing 400 mL sterilized YPD medium. The second inoculum culture was then incubated under the same condition as the first inoculum culture for 12 h.

Fermentation Scale-up

The BSM (3 L) was inoculated with 10% (v/v) second inoculum into a 5-L bioreactor (BIOTECH-5BG, Baoxing Co., Shanghai, China). The initial OD_{600} of the culture in bioreactor was about 0.5. A four-phase fermentation protocol (glycerol batch, glycerol fed-batch, starvation period and constant-rate methanol feeding) was used. The glycerol or methanol feeding to the bioreactor was controlled by a pump. The bioreactor was operated at 30 °C and pH around 6.0 via adding 28% v/v ammonia. Dissolved O_2 cascade was constantly maintained above 30% air saturation.

Once glycerol was depleted from culture broth, indicated by a sharp increase in DO, the glycerol fed-batch phase was started at a constant flow rate of 18 mL/(L·h) with 50% (v/v) glycerol until the biomass reached about 180 g/L (wet cell density). After 1 h starvation period following the above high cell density fermentation, the culture was supplied with 100% (v/v) methanol to induce lipase expression and linearly ramped to maximum methanol feeding rates of 2, 3, 4 and 5 mL/(L·h) with an increasing rate of 1 mL/(L·h). Samples were taken at regular intervals to monitor the biomass, total protein concentration, lipase activity and alcohol oxidase activity.

Biomass, Total Protein Concentration, Lipase Activity, Alcohol Oxidase Activity

WCD of the cell suspension was determined by centrifugation of 10 mL cell broth in a pre-weighed centrifuge tube at 8000 × *g* at 4 °C for 10 min, and the fermentation supernatant was collected and used

for subsequent experiments. Total protein concentration in the supernatant was determined by the Bradford assay [29]. The activity of lipase MAS1 in supernatant was determined by alkali titration method using olive oil as substrate [30]. Olive oil (Macklin, Shanghai, China) was emulsified with 4% (w/v) polyvinyl alcohol at the ratio of 1:3 (v/v). Each reaction contained 4 mL of emulsified olive oil, 5 mL of phosphate buffer at 50 mM and pH 6.0 and 1 mL of enzyme solution, and was carried out at 65 °C. The reaction was terminated by adding 15 mL of 95% (v/v) ethanol. The released fatty acids were neutralized by 0.05 M NaOH. One unit of lipase activity is defined as the amount of enzyme releasing 1 μmol of fatty acid per minute. The AOX activity was determined using a previously reported method [31].

Cell Viability And Cell Death

The cell viability was measured using methylene blue dye exclusion technique [32]. The fresh fermentation broth was diluted and mixed with 0.1% (w/v) methylene blue in equal volume. After standing at room temperature for 10 min, the cells were observed under a microscope (MLS1, Mshot, China) through hemocytometer. To determine the effect of constant methanol feeding rate on cell death, cells were collected at the time point corresponding to the maximum enzyme activities, washed with PBS buffer (100 mM, pH6) and suspended in the same buffer (10^6 cells). Cell death was determined by propidium iodide staining kit (Sangon, Shanghai, China) with a fluorescence microscope (LSM800, ZEISS, Jena, Germany).

ROS detection

Cells were collected at the time point corresponding to the maximum enzyme activities, washed with PBS buffer and suspended in the same buffer (10^6 cells). Cell suspension (500 μL) was mixed with 2', 7'-dichlorofluorescein diacetate (DCFH-DA, dissolved in ethanol, Sigma, Missouri) to a final concentration of 10 μg/mL followed by incubation at 30 °C for 30 min. The cells were collected and washed twice with PBS buffer, and the fluorescence density (FLU) was measured by a fluorescent plate reader (CytoFLEX, Beckman coulter, Brea, CA) under excitation wavelength at 488 nm and emission wavelength at 520 nm. The relative fluorescence density (RFLU) was also calculated as the fluorescence density divided by the number of cells examined [26].

$O_2^{\bullet-}$, H_2O_2, SOD, CAT and GSH assays

Cells were collected at the time point corresponding to the maximum enzyme activities. The H_2O_2 content was calculated by measuring the absorbance at 390 nm. The cells were suspended in 3% trichloroacetic acid solution (2.5 mL), and centrifuged at 12000 × *g* and 4 °C for 10 min. Then 1 mL of the supernatant was mixed with equal volume of PBS buffer (pH 7), followed by adding 2 mL 1 mol/L potassium iodide.

The cells were resuspended in PBS buffer (50 mM, pH 7.8) containing 1 mmol/L EDTA and 1% (v/v) PVP, sonicated and then centrifuged at 12000 × *g* and 4 °C for 10 min. The supernatant was used for $O_2^{\bullet-}$, sSOD activity and CAT activity analysis, and protein concentration in the supernatant was determined by

the Bradford assay. The effect of constant methanol feeding rate on $O_2^{\bullet-}$ content was measured by determining nitrite production [33]. SOD activity, CAT activity and GSH content were determined by their cellular analysis kits, respectively (Nanjing Jiancheng BioENG, Co., Nanjing, China).

Determination of lipid peroxidation

Cells were collected at the time point corresponding to the maximum enzyme activities, washed with PBS buffer and suspended in the same buffer. MDA was quantified by measuring thiobarbituric acid reactive substances as described previously [34]. The cell suspension treated with snailase and digestion buffer (Sangon Biotech, shanghai, China) were centrifuged at 10,000 × *g* for 15 min at 4 °C. One volume of the supernatant was mixed with two volumes of TBA reactive (0.25 M chlorhydric acid, 15% (v/v) trichloroacetic acid and 0.375% (w/v) thiobarbituric acid). Subsequently, the samples were incubated for 20 min at 100 °C in a dry bath, and then the mixture was cooled on ice and centrifuged at 12,000 × *g* for 30 s at 4 °C. Supernatant absorbance was measured at 532 nm.

RNA isolation and quantitative real-time PCR (RT-qPCR)

Cells were collected at the time point corresponding to the maximum enzyme activities. Total yeast RNA was extracted using RNAiso Plus (Takara, Dalian, China) according to the manufacturer's instructions. The cDNA was synthesized using PrimeScript™ RT reagent Kit with gDNA Eraser (Takara, Dalian, China). RT-qPCR was conducted in CFX96 Real-Time PCR Detection System (Bio-Rad, Hercules, CA), and SYBR Green PCR Master Mix kit (Takara, Dalian, China) was used for the real-time PCR analysis. The primers used for RT-qPCR are listed in Table 2. The relative expressions of target genes were calculated by the $2^{-\Delta\Delta Ct}$ method [35].

Table 2
List of primers used to amplify mRNA by quantitative qRT-PCR

Gene	Forward primer (5'-3')	Reverse primer (5'-3')
Actin	GTCCAGCATAAACACGCCG	CAGTGGGAAAAACCCACGAA
cSOD	CGAACAATCCTCCGAAAG	ACCCTTGGCAACACCTTCA
mSOD	AAACAAGGAGGTGGAGAGC	CAAAGGGACCAAACTACC
CAT	GCTACTAACCTGAAGGACGC	TTGAAGTTTACGACACCCAG
GPX1	CCCATTAGATAAGAAAGGCG	CCAAACTGGTTACAGGGAA
GLR1	AACTTCGCCCAACCGTAT	TCTCAATCGCCAAGGACT

Abbreviations

ROS: Reactive oxygen species; WCD: Wet cell density; AOX: Alcohol oxidase; SOD: Superoxide dismutase; CAT: Catalase; GSH: Reduced glutathione; MDA: Malondialdehyde; cSOD: Cytosolic superoxide

dismutase; mSOD: Mitochondrial superoxide dismutase; GPX: Glutathione peroxidise; GLR: Glutathione reductase; YPD: Yeast extract peptone dextrose; BSM: Basal salt medium; FLU: Fluorescence density; RFLU: Relative fluorescence density.

Declarations

Authors' contributions

YW and DL designed the experiments. RH, DL, RC, HH, YN and YW participated in the discussion about the experiments. RH performed experiments and drafted the manuscript. All authors read and approved the fnal manuscript.

Acknowledgements

Not applicable.

Funding

This work was supported by the National Key R & D Program of China (2018YFC0311104), National Science Fund for Distinguished Young Scholars (31725022), Key Program of Natural Science Foundation of China (31930084) and Guangdong marine economy promotion projects (MEPP) Fund (no. GDOE[2019]A20).

Availability of data and materials

The data sets supporting the conclusions of this article are included within the article.

Ethics approval and consent to participate

Not applicable.

Consent for publication

Not applicable.

Competing interests

The authors declare that they have no competing interests.

References

1. Shang T, Si D, Zhang D, Liu X, Zhao L, Hu C, Fu Y, Zhang R. Enhancement of thermoalkaliphilic xylanase production by *Pichia pastoris* through novel fed-batch strategy in high cell-density fermentation. Bmc Biotechnol. 2014;17**:**311-316.

2. Calik P, Bayraktar E, Inankur B, Soyaslan ES, Sahin M, Taspinar H, Ozdamar TH. Influence of pH on recombinant human growth hormone production by *Pichia pastoris*. J. Chem. Technol. Biot. 2010;85:1628-1635.
3. Wang J, Wu Z, Zhang T, Wang Y, Yang B. High-level expression of *Thermomyces dupontii* thermophilic lipase in *Pichia pastoris* via combined strategies. 3 Biotech. 2019;9:1-9.
4. Su X, Geng X, Fu M, Wu Y, Yin L, Zhao F, Chen W. High-level expression and purification of a Mollusca endoglucanase from *Ampullaria crossean* in *Pichia pastoris*. Protein Expres. Purif. 2017;139:8-13.
5. Yu Y, Zhou X, Wu S, Wei T, Yu L. High-yield production of the human lysozyme by *Pichia pastoris* SMD1168 using response surface methodology and high-cell-density fermentation. Electron. J. Biotechn. 2014;17:311-316.
6. Steels EL, Learmonth RP, Watson K. Stress tolerance and membrane lipid unsaturation in *Saccharomyces cerevisiae* grown aerobically or anaerobically. Microbiology. 1994;140:569-576.
7. Zhang W, Bevins MA, Plantz BA, Smith LA, Meagher MM. Modeling *pichia pastoris* growth on methanol and optimizing the production of a recombinant protein, the heavy-chain fragment C of botulinum neurotoxin, serotype a. Biotechnol. Bioeng. 2000;70:1-8.
8. Kupcsulik B, Sevella B, Ballagi A, Kozma J. Evaluation of three methanol feed strategies for recombinant *Pichia pastoris* MutS fermentation. Acta Aliment. 2001;30:99-111.
9. Wu D, Zhu H, Chu J, Wu J. N-acetyltransferase co-expression increases α-glucosidase expression level in *Pichia pastoris*. J. Biotechnol. 2019;289:26-30.
10. Gao M, Dong S, Yu R, Wu J, Zheng Z, Shi Z, Zhan X. Improvement of ATP regeneration efficiency and operation stability in porcine interferon-αproduction by *Pichia pastoris* under lower induction temperature. Korean J. Chem. Eng. 2011;28:1412-1419.
11. Gao M, Li Z, Yu R, Wu J, Zheng Z, Shi Z, Zhan X, Lin C. Methanol/sorbitol co-feeding induction enhanced porcine interferon-α production by *P. pastoris* associated with energy metabolism shift. Bioproc. Biosyst. Eng. 2012;35:1125-1136.
12. Gellissen G: Heterologous protein production in methylotrophic yeasts. Appl. Microbiol. Biot. 2000;54:741-750.
13. Qiu Z, Liu X, Tian X, Yue M. Effects of CO_2 laser pretreatment on drought stress resistance in wheat. J. Photoch. Photobio. B. 2008;90:17-25.
14. Vanz AL, Lünsdorf H, Adnan A, Nimtz M, Gurramkonda C, Khanna N, Rinas U. Physiological response of *Pichia pastoris* GS115 to methanol-induced high level production of the Hepatitis B surface antigen: catabolic adaptation, stress responses, and autophagic processes. Microb. Cell Fact. 2012;11:103-113.
15. Haynes CM, Titus EA, Cooper AA. Degradation of misfolded proteins prevents er-derived oxidative stress and cell death. Mol. Cell. 2004;15:767-776.
16. Schwarzhans J, Luttermann T, Geier M, Kalinowski J, Friehs K. Towards systems metabolic engineering in *Pichia pastoris*. Biotechnol. Adv. 2017;35:681-710.

17. Wei C, Zhou X, Zhang Y. Improving intracellular production of recombinant protein in *Pichia pastoris* using an optimized preinduction glycerol-feeding scheme. Appl. Microbiol. Biot. 2008;78:257-264.
18. Barrigón JM, Montesinos JL, Valero F. Searching the best operational strategies for *Rhizopus oryzae* lipase production in *Pichia pastoris* Mut^+ phenotype: Methanol limited or methanol non-limited fed-batch cultures? Biochem. Eng. J. 2013;75:47-54.
19. Dan W, Chu J, Hao Y, Wang Y, Zhuang Y, Zhang S. High efficient production of recombinant human consensus interferon mutant in high cell density culture of *Pichia pastoris* using two phases methanol control. Process Biochem. 2011;46:1663-1669.
20. Lee J, Won Y, Park K, Lee M, Tachibana H, Yamada K, Seo K. Celastrol inhibits growth and induces apoptotic cell death in melanoma cells via the activation ROS-dependent mitochondrial pathway and the suppression of PI3K/AKT signaling. Apoptosis. 2012;17:1275-1286.
21. Costa VMV, Amorim MA, Quintanilha A, Moradas-Ferreira P. Hydrogen peroxide-induced carbonylation of key metabolic enzymes in *Saccharomyces cerevisiae*: the involvement of the oxidative stress response regulators Yap1 and Skn7. Free Radical Bio. Med. 2002;33:1507-1515.
22. Halliwell B, Gutteridge JMC: *Free radicals in biology and medicine.* Fifth edn. Oxford, United Kingdom: Oxford University Press. 1985.
23. Fahey, C. R. Novel Thiols of Prokaryotes. Annu. Rev. Microbiol. 2001;55:333-356.
24. Delic M, Rebnegger C, Wanka F, Puxbaum V, Haberhauer-Troyer C, Hann S, K?llensperger G, Mattanovich D, Gasser B. Oxidative protein folding and unfolded protein response elicit differing redox regulation in endoplasmic reticulum and cytosol of yeast. Free Radical Bio. Med. 2012;52:2000-2012.
25. Tessoulin B, Descamps G, Moreau P, Maiga S, Lode L, Godon C, Marionneau-Lambot S, Oullier T, Le Gouill S, Amiot M, Pellat-Deceunynck C. PRIMA-1(Met) induces myeloma cell death independent of p53 by impairing the GSH/ROS balance. Blood. 2014;124:1626-1636.
26. Liu Z, Zhang M, Han X, Xu H, Zhang B, Yu Q, Li M. TiO_2 nanoparticles cause cell damage independent of apoptosis and autophagy by impairing the ROS-scavenging system in *Pichia pastoris*. Chem.-Biol. Interact. 2016;252:9-18.
27. Lan D, Qu M, Yang B, Wang Y. Enhancing production of lipase MAS1 from marine *Streptomyces* sp. strain in *Pichia pastoris* by chaperones co-expression. Electron. J. Biotechn. 2016;22:62-67.
28. Yuan D, Lan D, Xin R, Yang B, Wang Y. Screening and characterization of a thermostable lipase from marine *Streptomyces* sp. strain W007. Biotechnol. Appl. Bioc. 2016;63:41-50.
29. Li H, Xia Y. High-yield production of spider short-chain insecticidal neurotoxin Tx4(6–1) in *Pichia pastoris* and bioactivity assays in vivo(Article). Protein Expres. Purif. 2019;154:66-73.
30. Zhang X, Ai Y, Xu Y, Yu X. High-level expression of *Aspergillus* niger lipase in *Pichia pastoris*: Characterization and gastric digestion in vitro. Food Chem. 2019;247:305-313.
31. Suye S-i, Ogawa A, Yokoyama S, Obayashi A. Screening and identification of Candida methanosorbosa as acohol oxidase-producing methanol using yeast. Agr. Biol. Chem. 1990;54:1297-

1298.

32. Sinha J, Plantz BA, Inan M, Meagher MM. Causes of proteolytic degradation of secreted recombinant proteins produced in methylotrophic yeast *Pichia pastoris*: case study with recombinant ovine interferon-tau. Biotechnol. Bioeng. 2010;89:102-112.
33. Liu T, Zhu L, Wang J, Wang J, Zhang J, Sun X, Zhang C. Biochemical toxicity and DNA damage of imidazolium-based ionic liquid with different anions in soil on Vicia faba seedlings. Sci. Rep. 2015;5:18444-18453.
34. Zepeda AB, Figueroa CA, Pessoa A, Farías JG. Free fatty acids reduce metabolic stress and favor a stable production of heterologous proteins in *Pichia pastoris*. Braz. J. Microbiol. 2018;49:856-864.
35. Livak K, Schmittgen T. Analysis of relative gene expression data using real-time quantitative PCR and the $2^{-\triangle\triangle Ct}$ method. Methods. 2000;25:402-408.

Figures

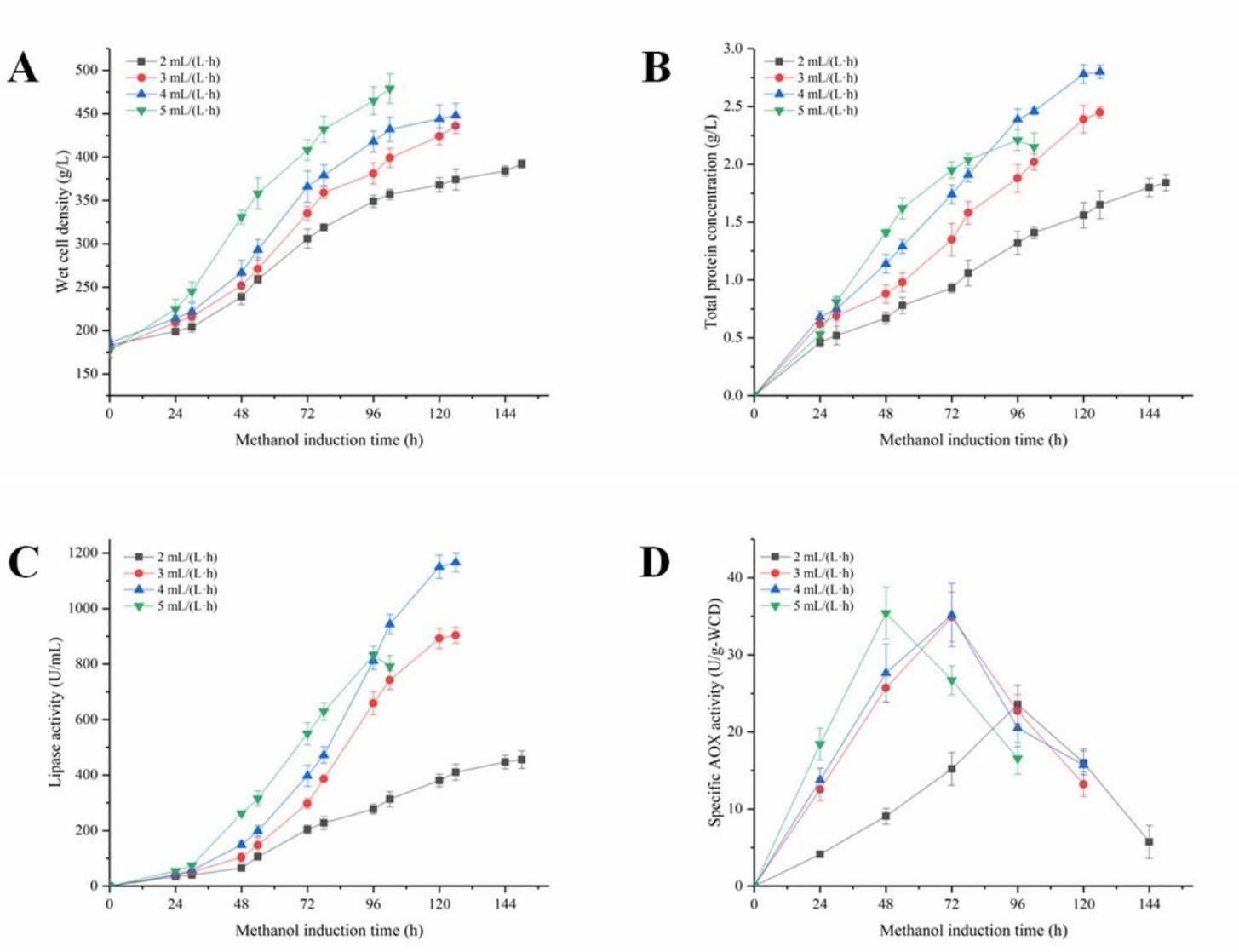

Figure 1

Effects of methanol feeding rates on the fermentation within the induction time. (A) Wet cell density, (B) total protein concentration, (C) lipase activity, and (D) specific alcohol oxidase activity. The error bars represent the results of the triplicate runs.

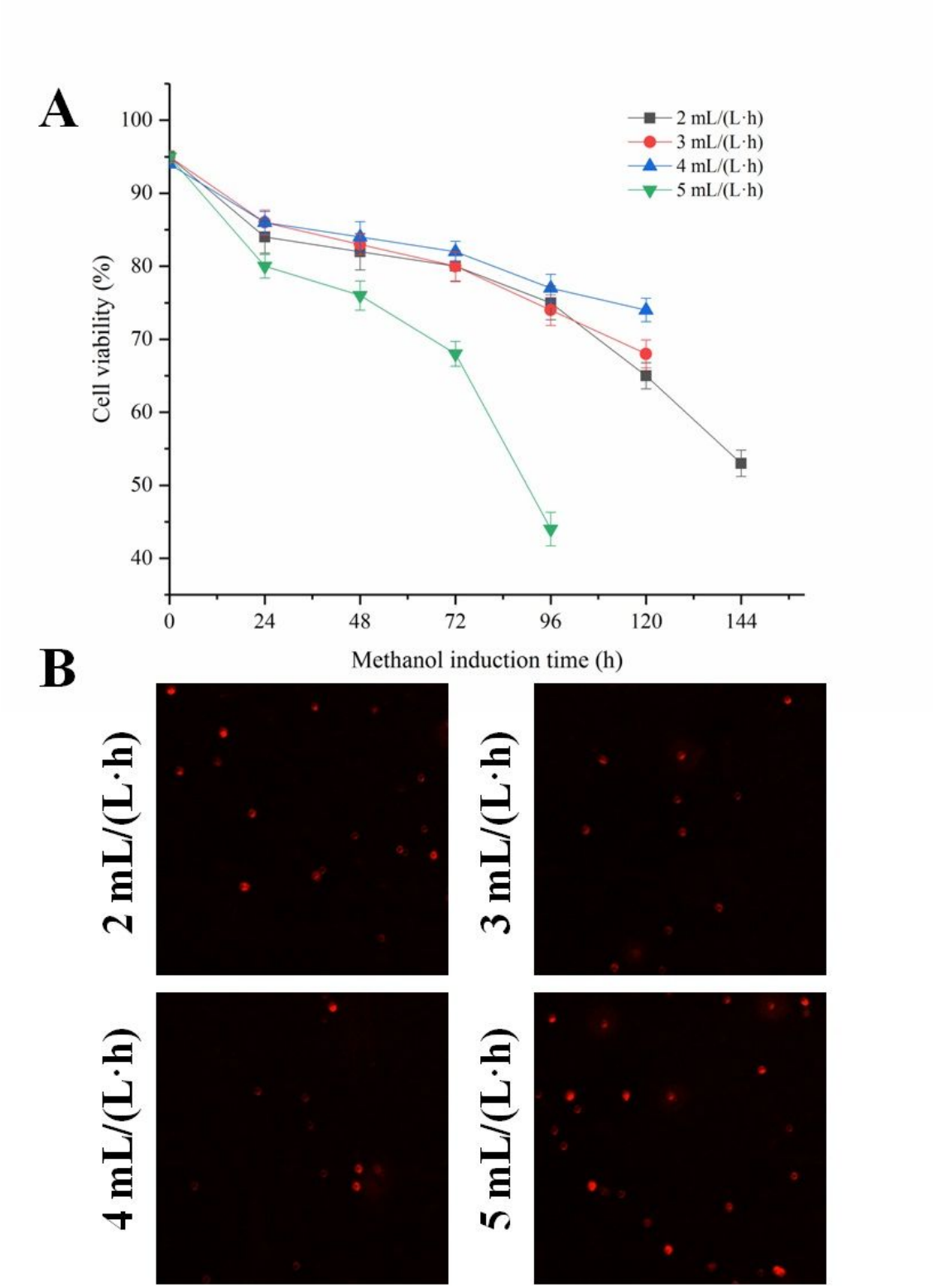

Figure 2

Effects of methanol feeding rates on cell viability and cell death. (A) Cell viability, and (B) cell death. The treated cells were stained with PI and observed by fluorescence microscopy. The percentage of propidium

iodide-positive cells was calculated by the number of propidium iodide-positive cells divided by that of total cells×100. Error bars are the SD value calculated from triple experiments.

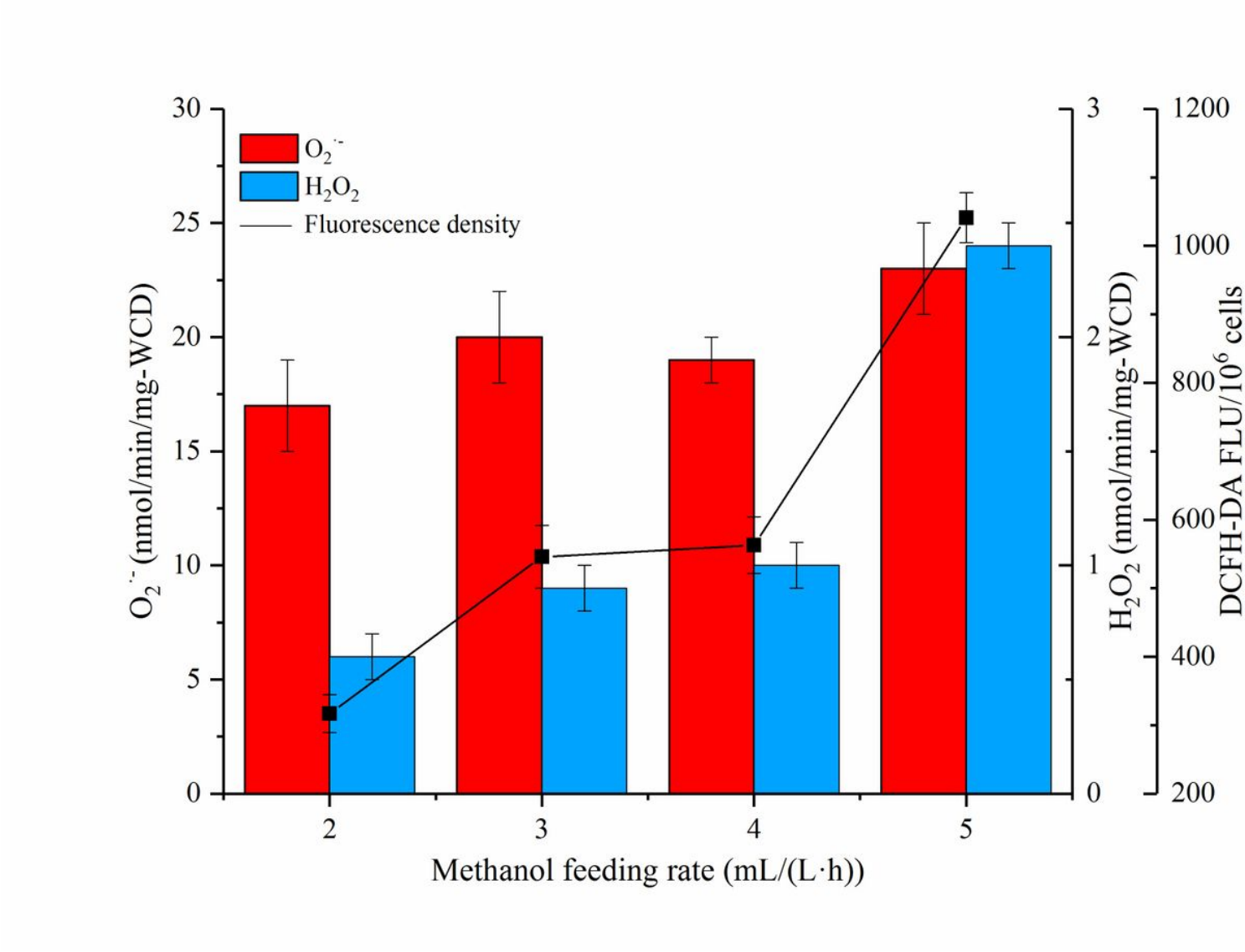

Figure 3

Effects of methanol feeding rates on reactive oxygen species (ROS) accumulation. Error bars are the SD value calculated from triple experiments.

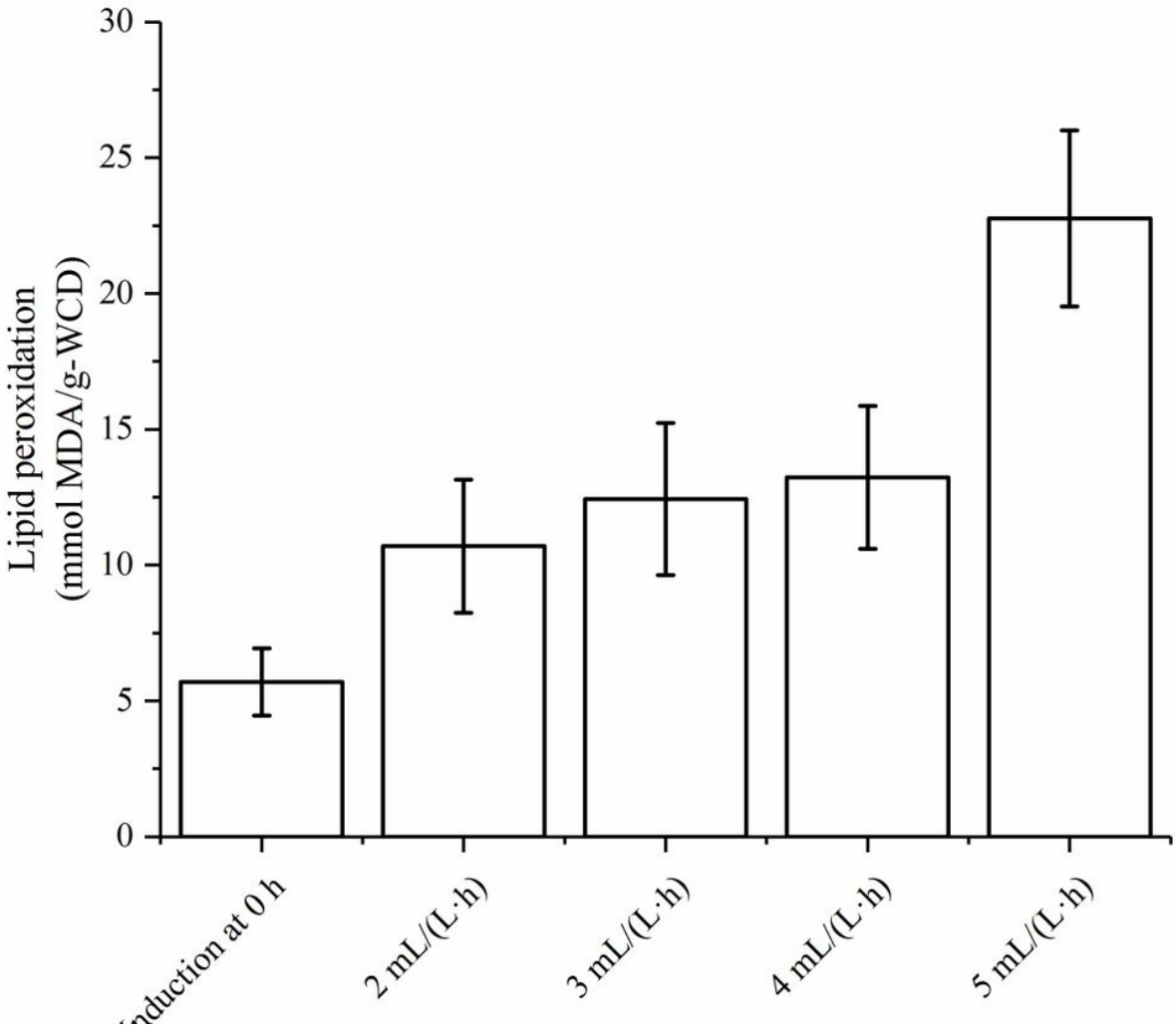

Figure 4

Effects of methanol feeding rates on lipid peroxidation levels. Error bars are the SD value calculated from triple experiments.

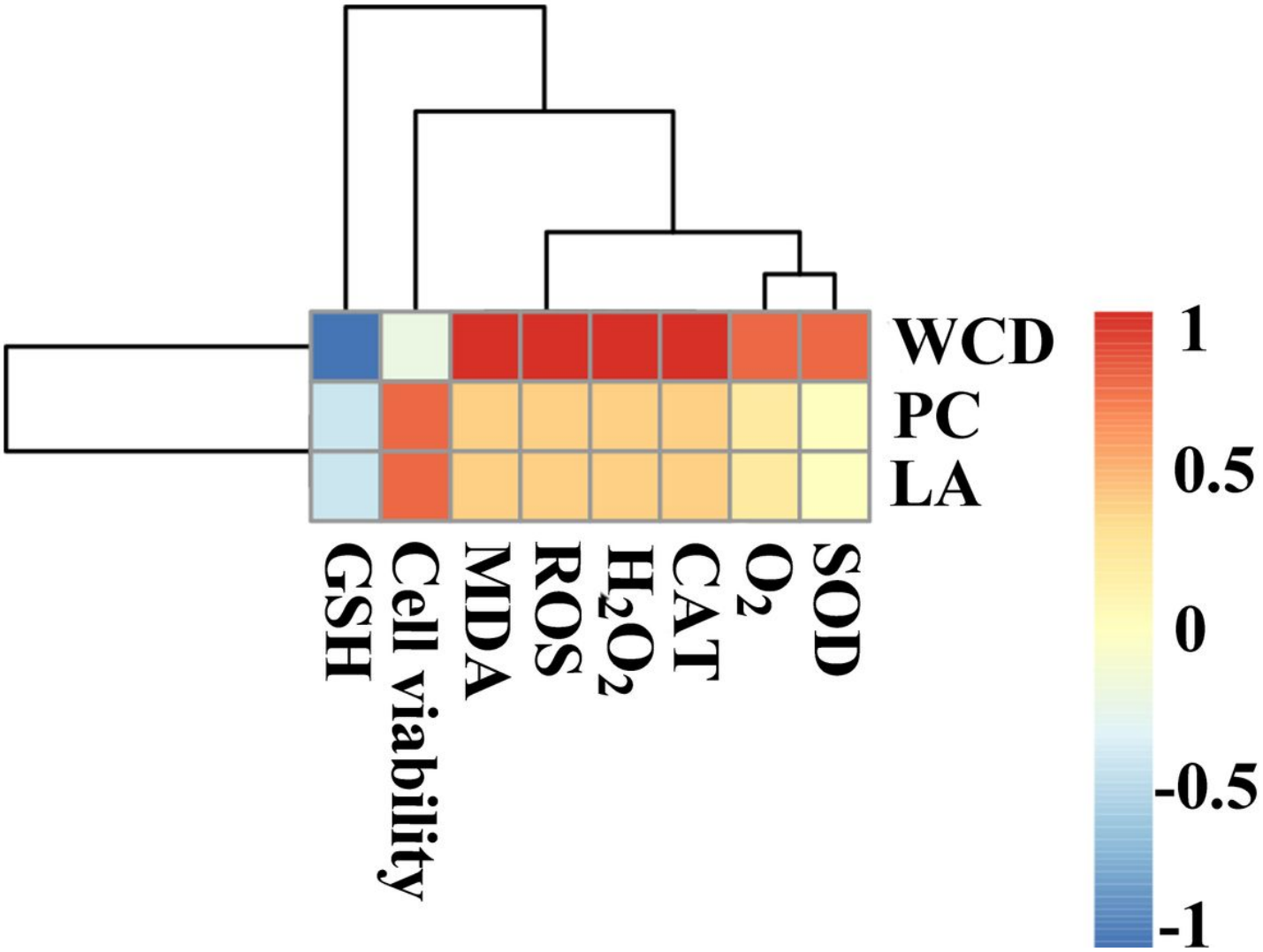

Figure 5

A Spearman's correlation heatmap was used to represent significant statistical correlation values (r) between fermentation performance and ROS-associated parameters with different methanol feeding rate. The intensity of the colour represents the degree of association between fermentation performance and ROS-associated parameters [numerical values: WCD: Wet cell density; PC: Total protein concentration; LA: Lipase activity].

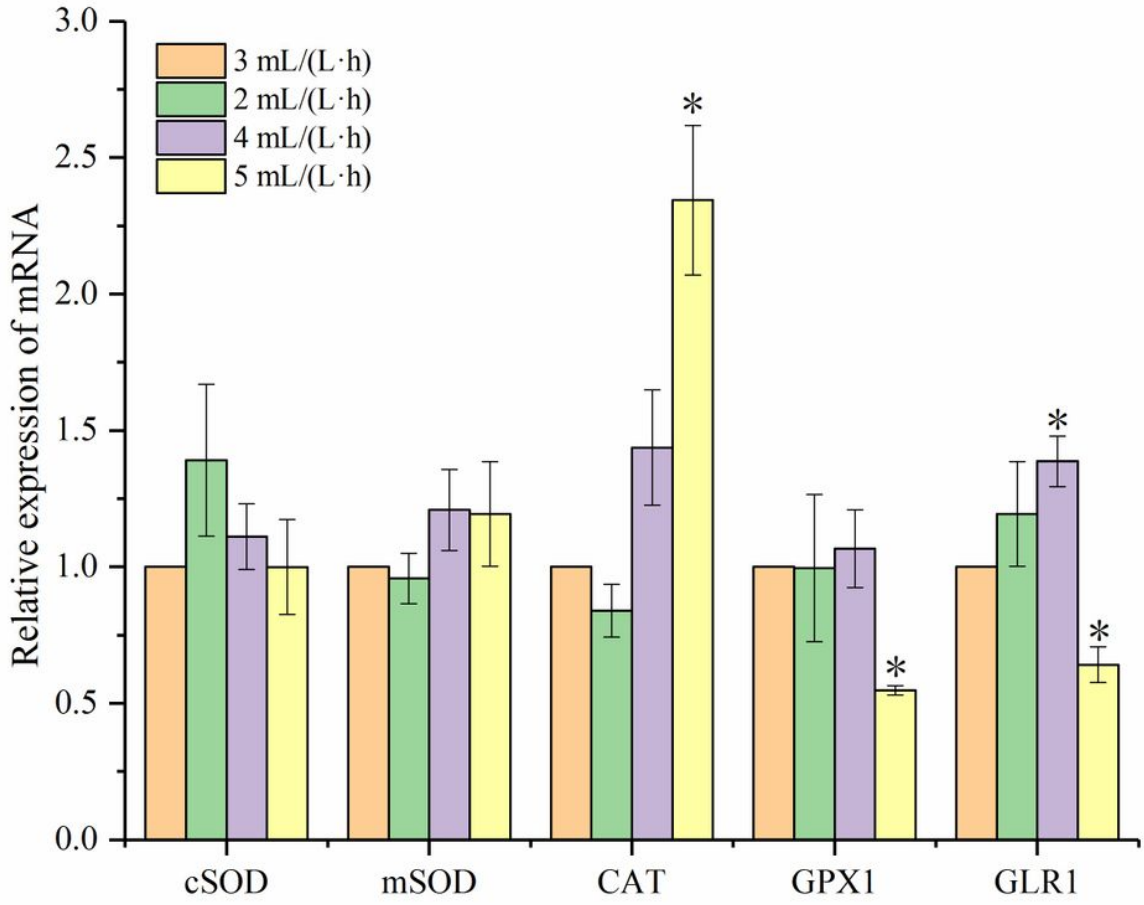

Figure 6

The expressions of genes at the mRNA levels were determined using RT-qPCR. Data were expressed as means ± SD. Differences were assessed by ANOVA and denoted as follows: *p < 0.05 versus methanol feeding rate of 3 mL/(L·h).